

Supporting Information for

Consideration of Binding Kinetics in the Design of Stapled Peptide Mimics of the Disordered Proteins Eukaryotic Translation Initiation Factor 4E (eIF4E)-Binding Protein 1 (4E-BP1) and Eukaryotic Translation Initiation Factor 4G (eIF4G)

Erin E. Gallagher[†], James M. Song[†], Arya Menon, Lauren D. Mishra, Alyah F. Chmiel, and Amanda L. Garner*

Department of Medicinal Chemistry, College of Pharmacy, and Program in Chemical Biology, University of Michigan, Ann Arbor, Michigan 48109, United States

[†]These authors contributed equally

A. Stapled Peptide Design	Pages S2–S3
B. Peptide Characterization Data	Pages S4–S6
C. Supplemental Figures	Pages S6–S16
D. Supplemental Tables	Pages S17–S21

A. Stapled Peptide Design

Analysis of the crystal structure of 4E-BP1 in complex with eIF4E (PDB: 1WKW; **Figure S1**) indicated that the helical portion of bound 4E-BP1 only spans 6 amino acids; therefore, an $i,i+7$ staple was not a possibility. Of the two possible staple sites, Arg56/Met60 and Lys57/Glu61, we noted that elimination of the Arg and Met side chains would disrupt a key salt bridge between Arg56 and Glu132 of eIF4E; therefore, Lys57/Glu61 was determined to be the optimal staple site. Similar sites were predicted for eIF4G using the same analysis (data not shown).

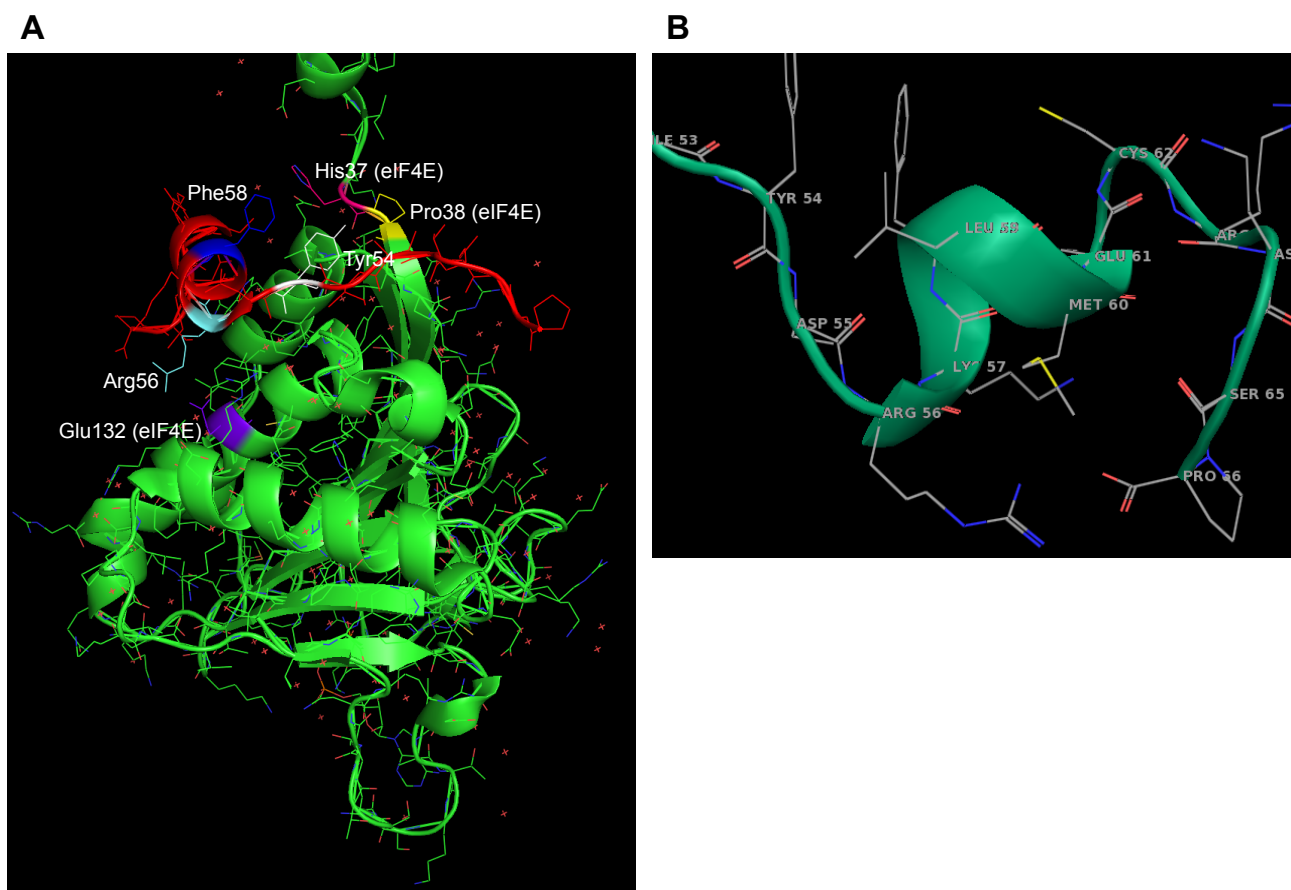


Figure S1. Structures of (A) eIF4E (green) bound to a 4E-BP1 peptide (red) (PDB: 1WKW), and (B) a zoomed-in view of the helical region of 4E-BP1.

To confirm that this would be optimal, we performed virtual sequential alanine mutagenesis and scored the docking pose of each resulting 4E-BP1 mutant peptide with eIF4E using Glide Score (Schrödinger LLC), an empirical scoring function that approximates ligand binding free energy. The score of each pose was then compared to the score of native 4E-BP1 in the same complex (**Figure S2**). To compare the effect of ligand sampling on the interaction, in one instance the mutant structure was allowed to minimize before the docking pose was assessed, while in the other, the structure was kept rigid. Our results showed that the software accurately predicted that Tyr54 and Leu59 are vital to the eIF4E–4E-BP1 PPI, in addition to suggesting that mutation of other sites (Arg51, Arg56) may negatively impact binding, as reported.³ Fortunately, our selected staple site, Lys57/Glu61, did not affect any of these positions.

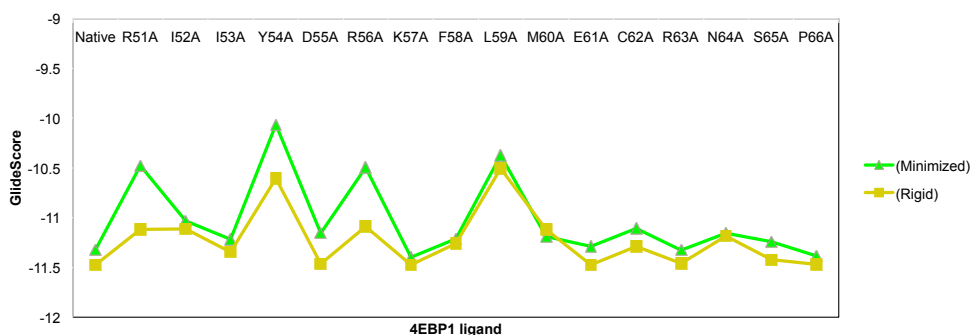


Figure S2. Virtual sequential alanine mutagenesis. The docking poses of each 4E-BP1 mutant peptide with eIF4E were analyzed against that of the native 4E-BP1 with eIF4E using Glide. A higher Glide Score indicates an unfavorable mutation, and therefore, a greater contribution to the ligand binding affinity.

Using amino acids Thr50–Asn64 as a peptide scaffold, additional docking analyses were performed (Maestro v9.7, Schrödinger LLC) to determine optimal staple length and stereochemistry. From these analyses, an 8-atom linker containing L-configuration alkenyl amino acids was predicted to be optimal (**Figure S3**).

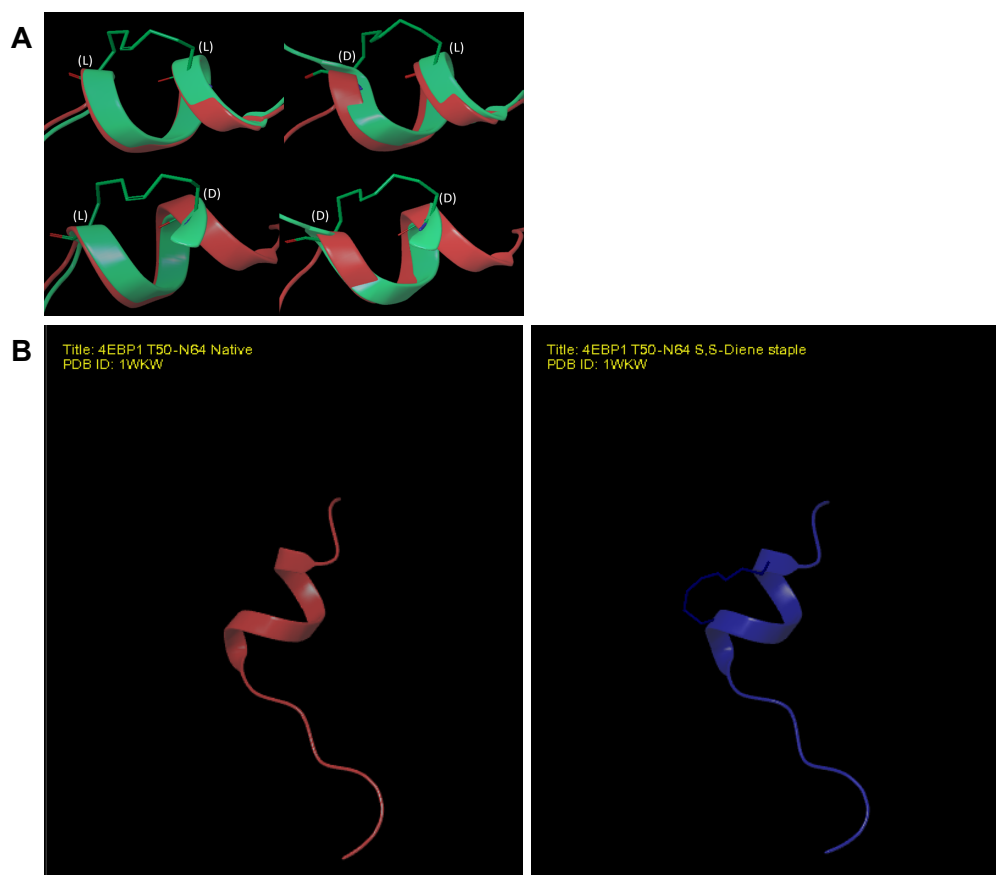
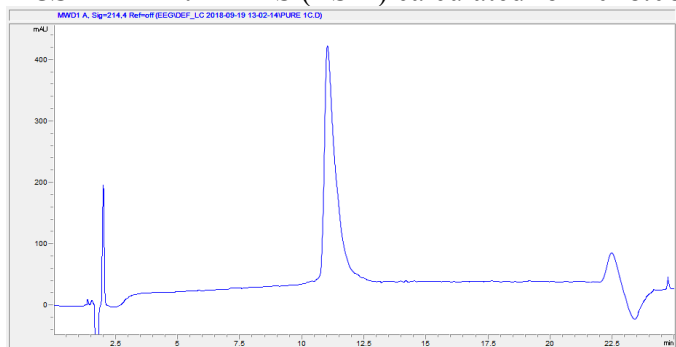


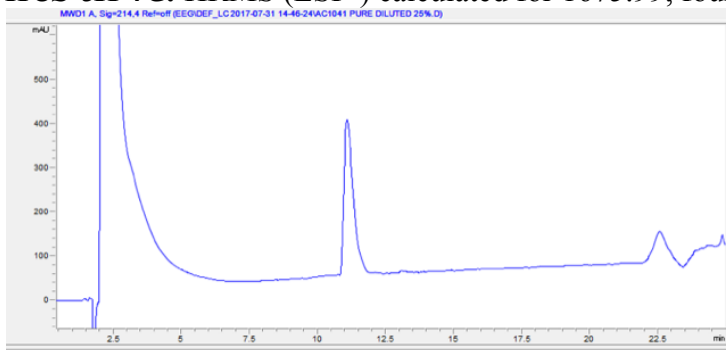
Figure S3. Determination of staple length and stereochemistry. (A) Alignment of docking poses of the 4E-BP1 native peptide (red) and predicted stapled peptides of varying stereochemistry (green). (B) Predicted structures of peptide **4E-BP1** (red) and **HCS-4E-BP1** (blue) showing little disruption of the helical structure upon stapling.

B. Peptide Characterization Data

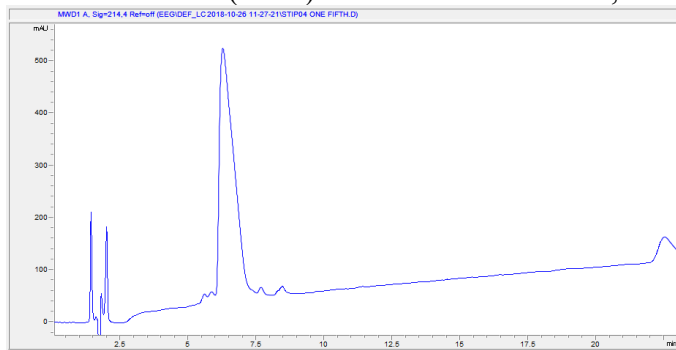
HCS-4E-BP1. HRMS (ESI+) calculated for 2048.08, found 2049.0969.



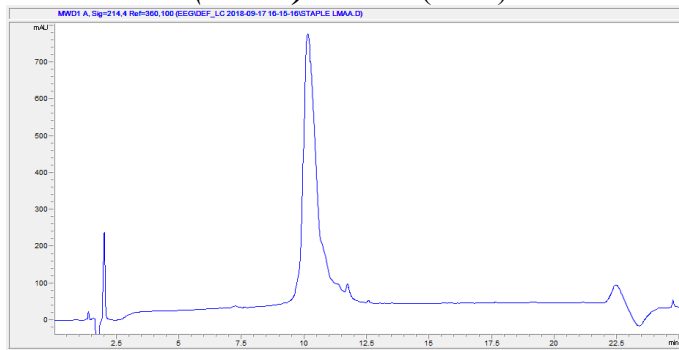
HCS-eIF4G. HRMS (ESI+) calculated for 1675.99, found 1676.9965.



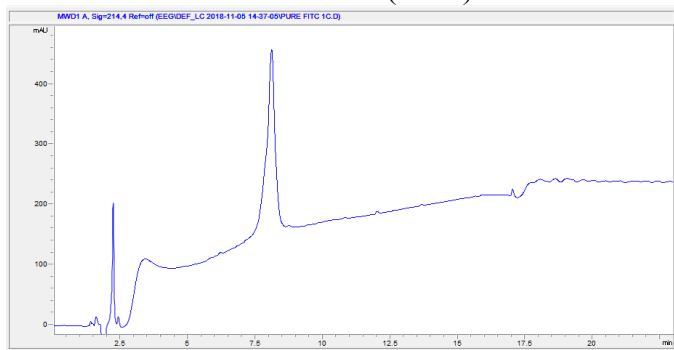
sTIP-04. HRMS (ESI+) calculated for 1595.00, found 1595.0079.



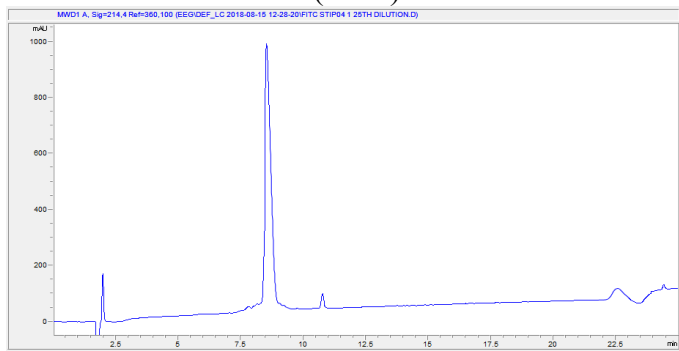
HCS-4E-BP1 (LMAA). HRMS (ESI+) calculated for 1946.03, found 1947.0506.



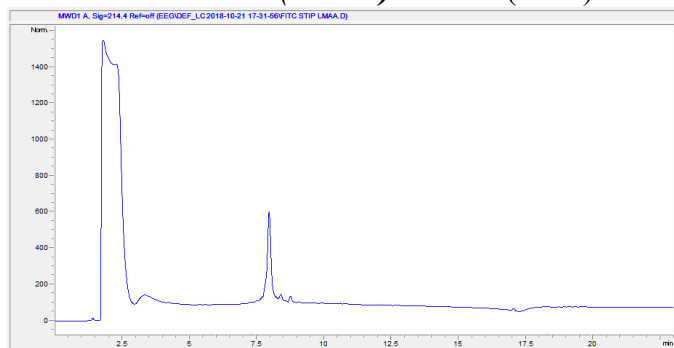
FITC-HCS-4E-BP1. HRMS (ESI+) calculated for 2540.18, found 2541.2112.



FITC-sTIP-04. HRMS (ESI+) calculated for 2087.10, found 2088.1088.



FITC-HCS-4E-BP1 (LMAA). HRMS (ESI+) calculated for 2438.13, found 2439.1408.



C. Supplemental Figures

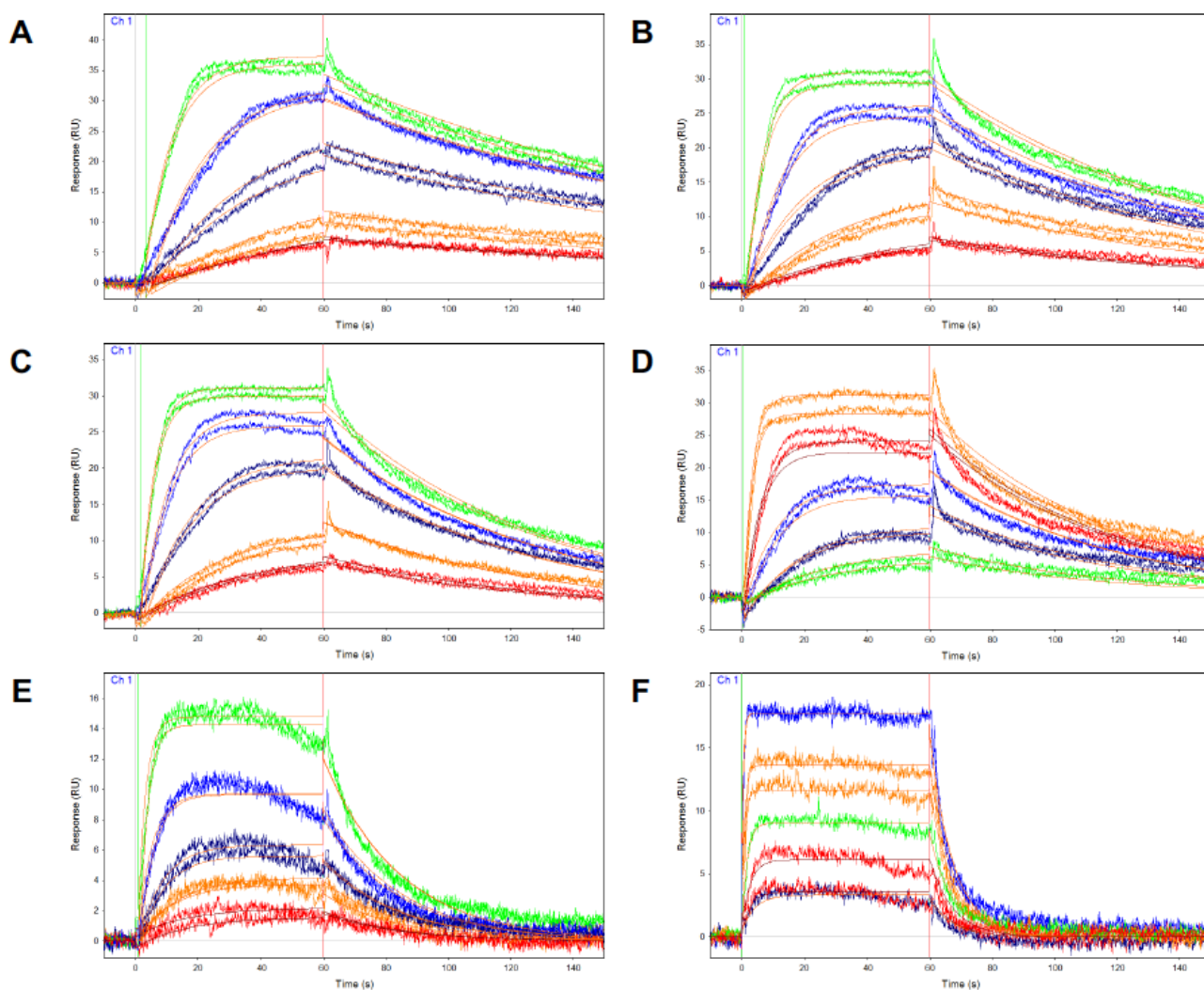


Figure S4. Linear 4E-BP1 peptide sensorgrams. (A)–(E) are representative sensorgrams for the linear 4E-BP1 peptide at 10, 15, 20, 25 and 30 °C from duplicate runs at varying concentrations (12.5, 25, 50, 100, 200 nM). (F) KKR-4E-BP1 peptide analysis as described above at 25 °C.

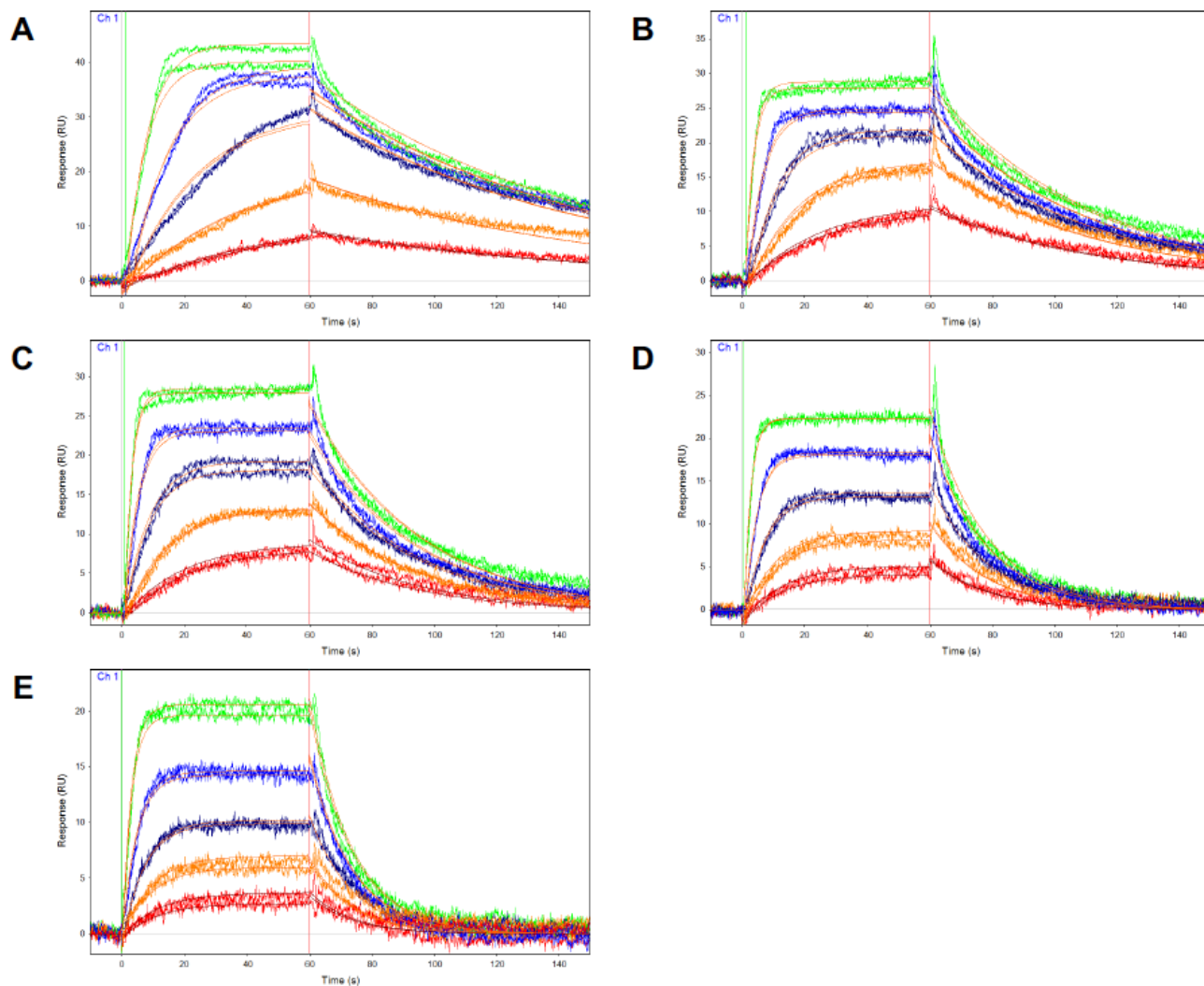


Figure S5. Linear eIF4G peptide sensorgrams. (A)–(E) are representative sensorgrams for the linear eIF4G peptide at 10, 15, 20, 25 and 30 °C from duplicate runs at varying concentrations (12.5, 25, 50, 100, 200 nM).

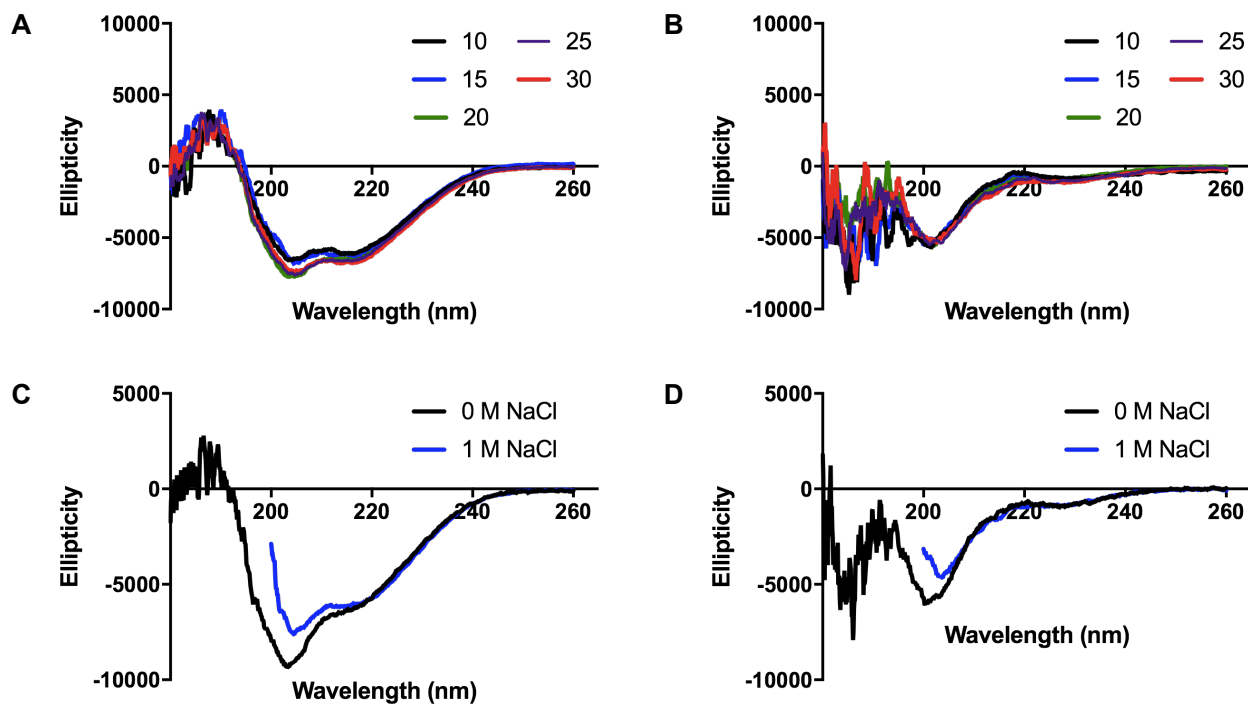


Figure S6. CD spectra of (A), (C) 4E-BP1 and (B), (D) eIF4G with respect to temperature (10–30 °C) or salt concentration (0 or 1 M). The average helicity of the 4E-BP1 peptide across temperatures was $17 \pm 2\%$; the eIF4G peptide was $2.5 \pm 0.5\%$. The average helicity of the 4E-BP1 peptide with respect to salt was $17 \pm 0.4\%$; the eIF4G peptide was $2.8 \pm 0.04\%$.

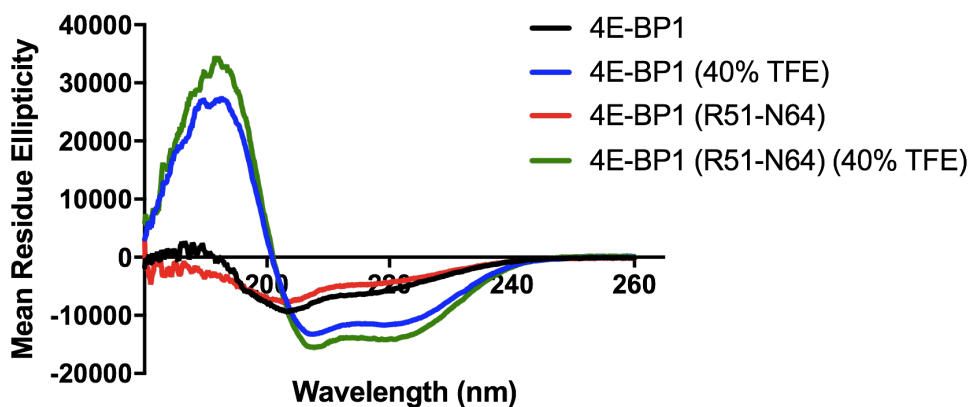


Figure S7. CD spectra of 4E-BP1 (R51–N64) in comparison to the 4E-BP1 peptide.

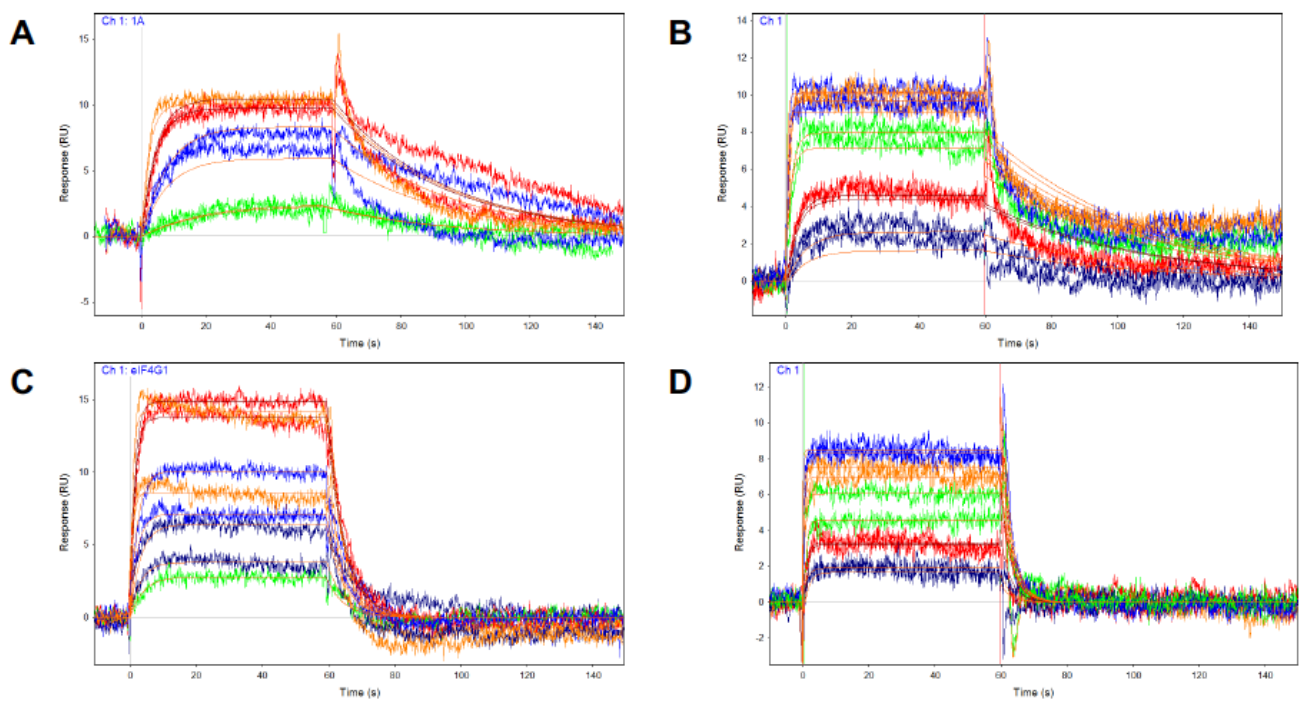


Figure S8. Representative linear 4E-BP1 and eIF4G peptide sensorgrams with (A), (C) 500 mM or (B), (D) 1000 mM NaCl, respectively, from duplicate runs.

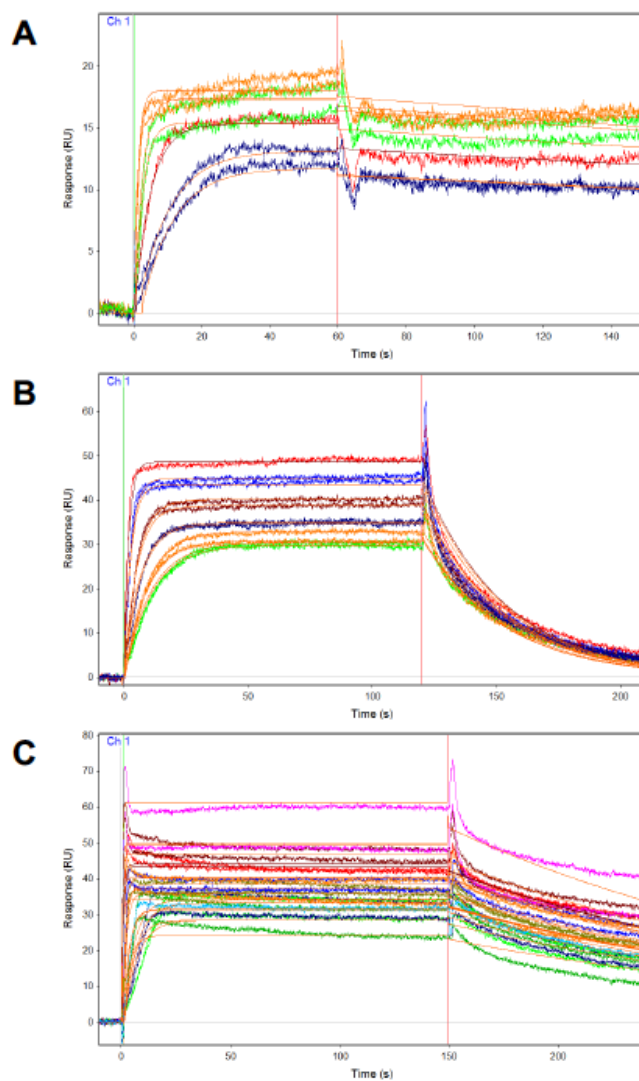


Figure S9. Representative sensorgrams for stapled peptides at 25 °C from duplicate runs at varying concentrations. (A) **HCS-4E-BP1** (62.5, 125, 250, 500 nM). (B) **HCS-eIF4G** (188, 250, 375, 500, 1000 nM). (C) **sTIP-04** (250, 375, 500, 750, 1000, 1500, 2000, 3000, 4000 nM).

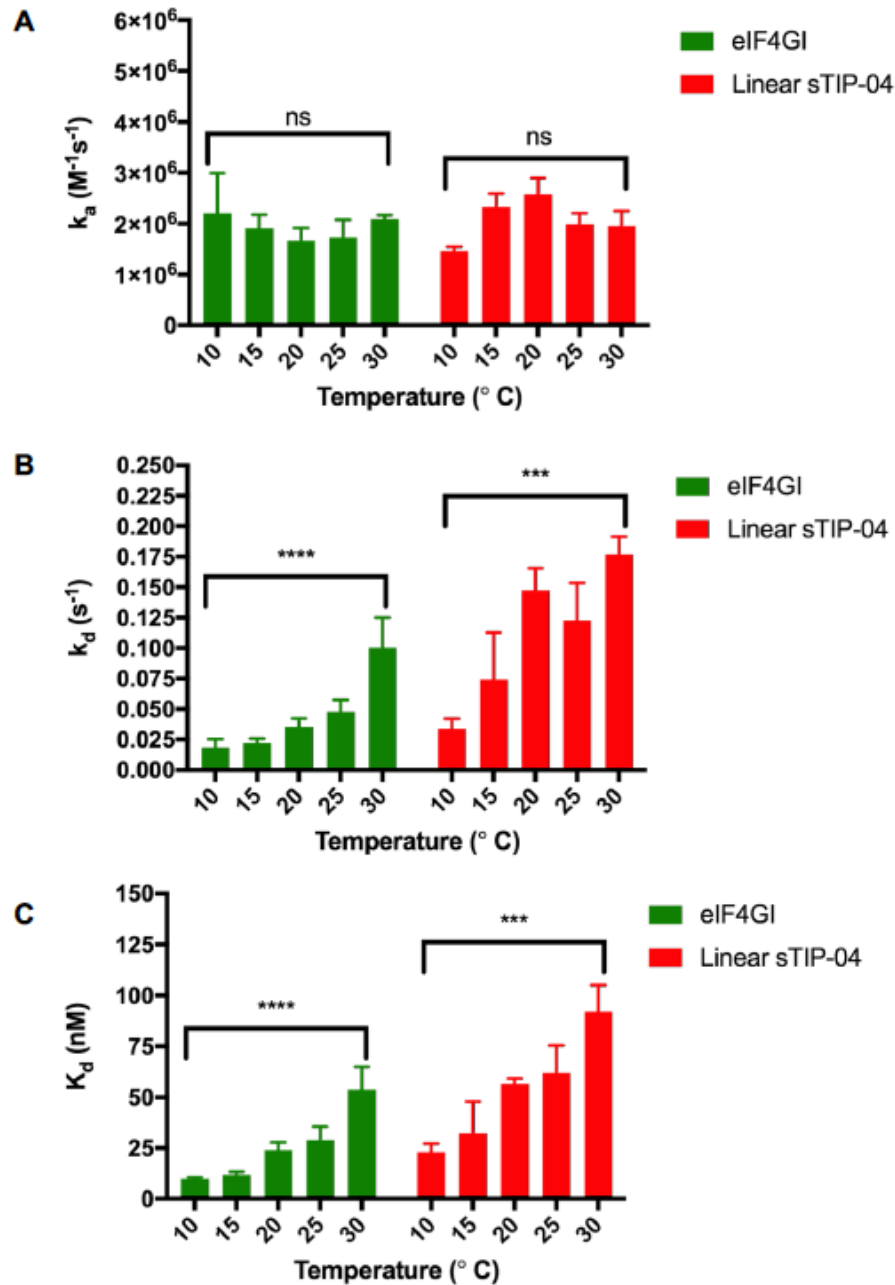


Figure S10. Kinetic analyses of eIF4G and **linear sTIP-04** peptides via SPR. The effect of temperature on (A) k_a , (B) k_d and (C) K_d . Statistical significance was determined using unpaired, two-tailed Student's *t* tests. ns = not significant ($p > 0.05$). p values for **linear sTIP-04** were as follows: 0.0517 (A), 0.0001 (B) and 0.0009 (C). Tabulated results can be found in Table S1.

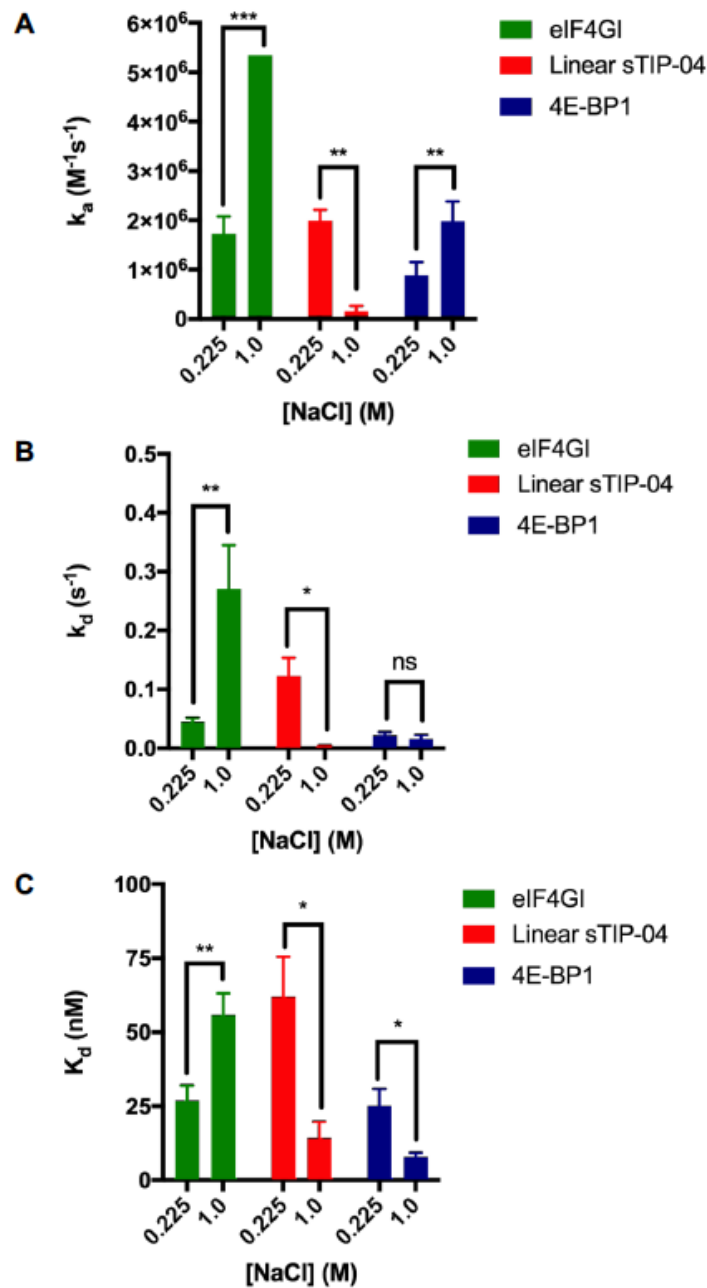


Figure S11. Kinetic analyses of eIF4G and **linear sTIP-04** peptides via SPR. The effect of salt on (A) k_a , (B) k_d and (C) K_d . Statistical significance was determined using unpaired, two-tailed Student's *t* tests. ns = not significant ($p > 0.05$). p values for **linear sTIP-04** were as follows: (A) 0.0018, (B) 0.0133, and (C) 0.0197. Tabulated results can be found in Table S4.

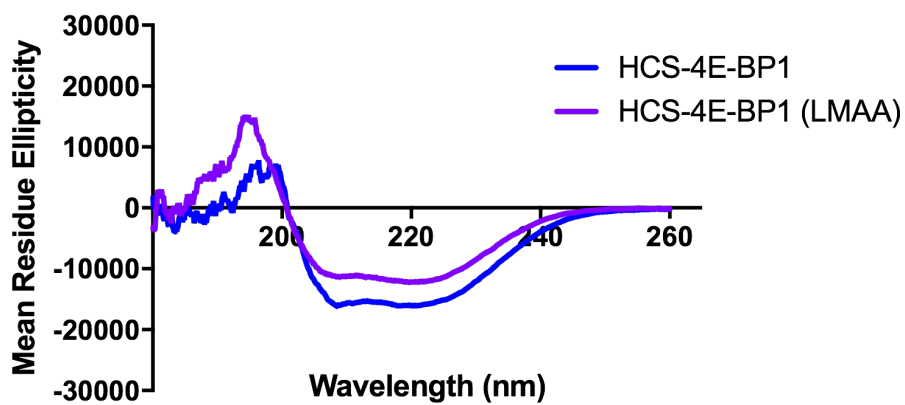


Figure S12. CD spectra of **HCS-4E-BP1 (LMAA)** in comparison to **HCS-4E-BP1**. Average helicity values measured at 25–100 μM \pm standard deviation are $35 \pm 3\%$ and $44 \pm 7\%$, respectively.

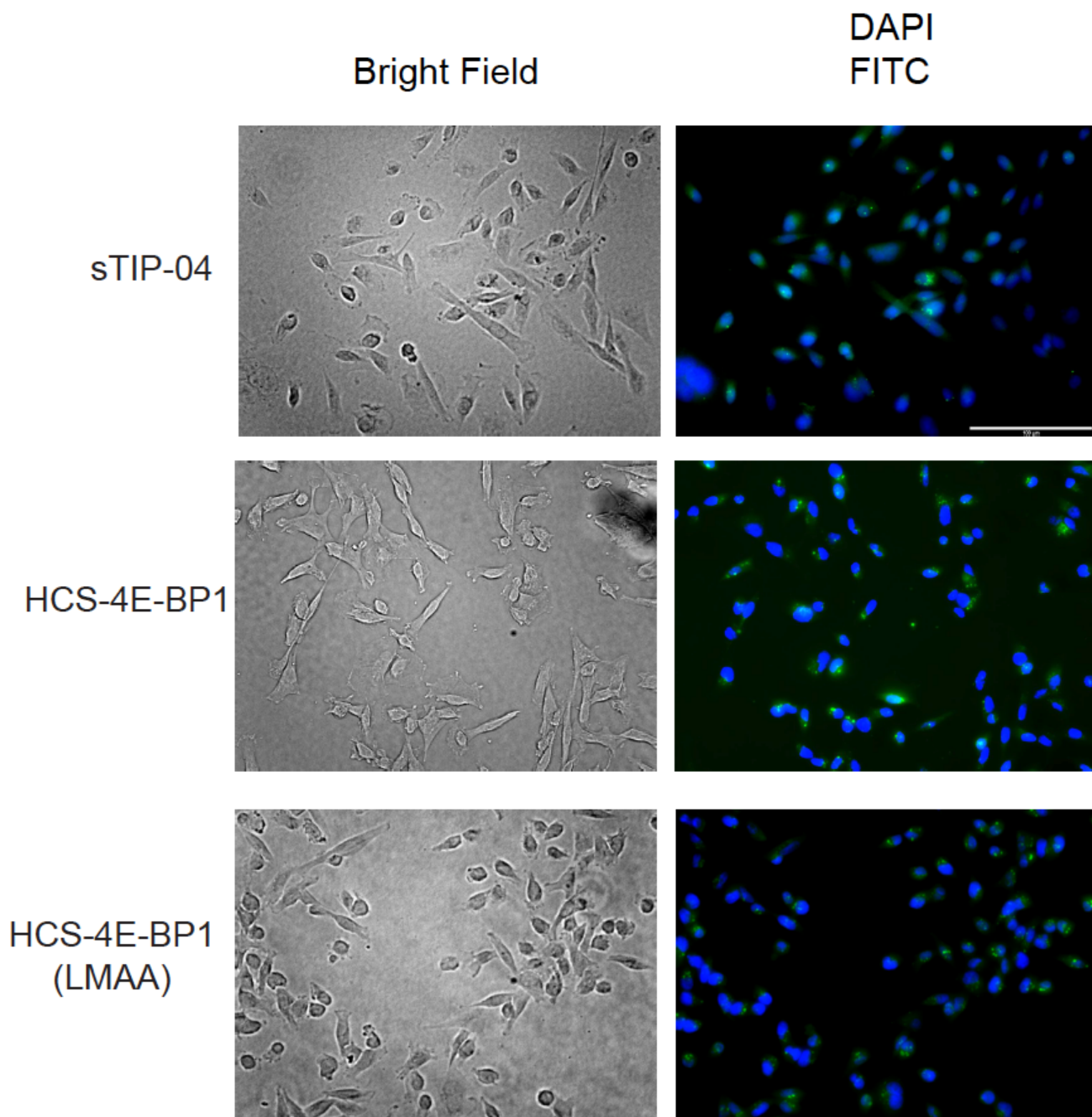


Figure S13. Cellular permeability of FITC-labeled **sTIP-04**, **HCS-4E-BP1** and **HCS-4E-BP1 (LMAA)** (1.0 μM) as determined via 20X imaging in MDA-MB-231 cells. The scale in the DAPI/FITC overlay for **sTIP-04** is 100 μm and is representative for the entire panel.

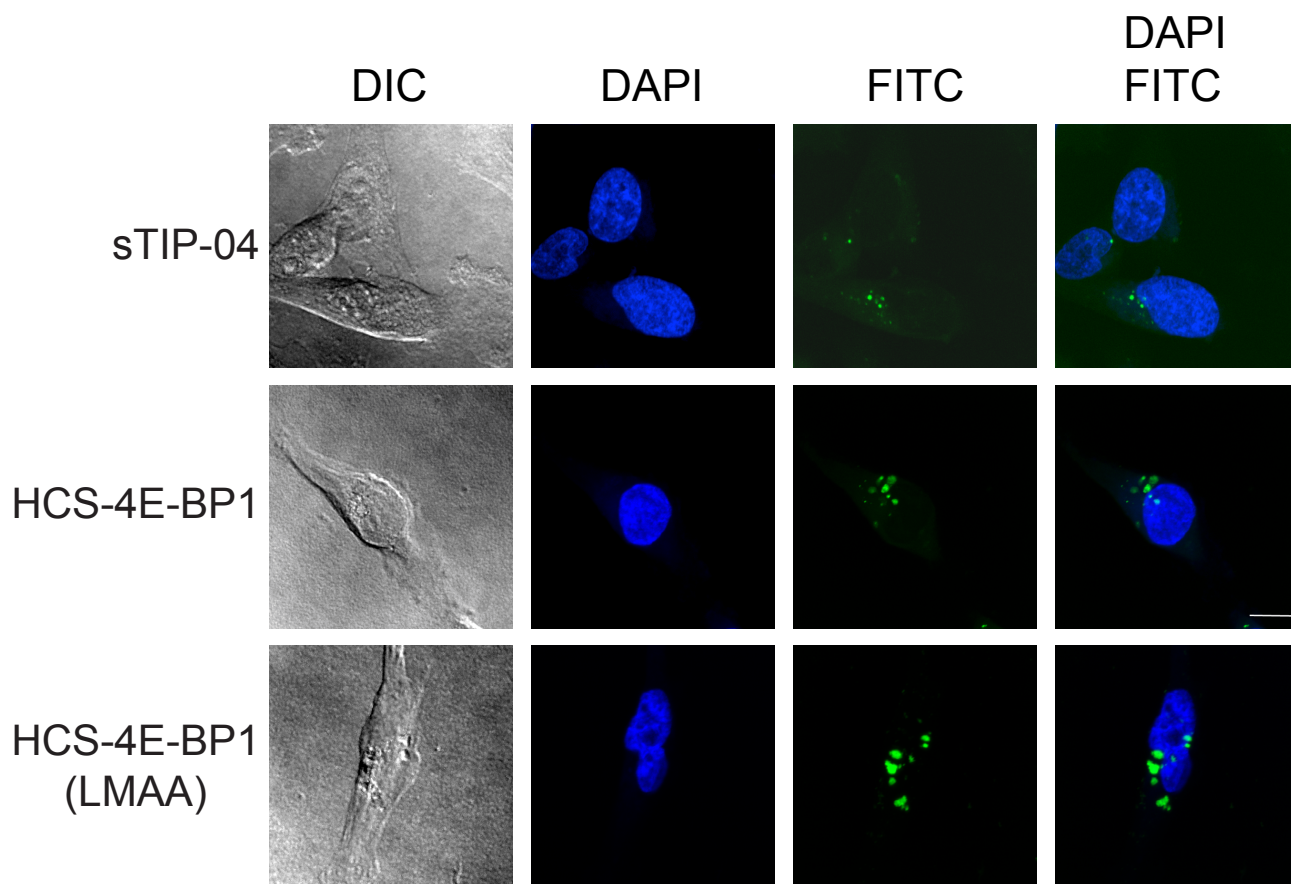


Figure S14. Cellular permeability of FITC-labeled **sTIP-04**, **HCS-4E-BP1** and **HCS-4E-BP1 (LMAA)** as determined via confocal microscopy in MDA-MB-231 cells. The scale in the DAPI/FITC overlay for **HCS-4E-BP1** is 10 μm and is representative for the entire panel.

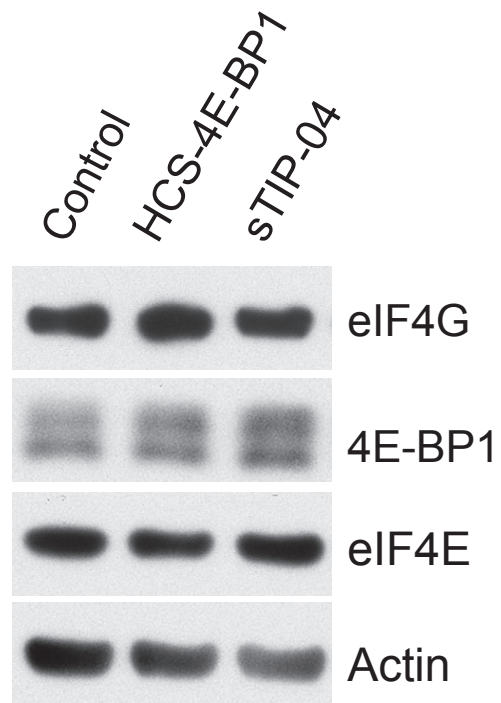


Figure S15. Western blot of total protein levels of eIF4G, 4E-BP1 and eIF4E following treatment with 5 μ M peptide for 6 h. Actin was used as a normalization control.

D. Supplemental Tables

Table S1. Tabulated SPR results from Figures 3 and S10

Peptide	Temperature (°C)	$k_a \times 10^6$ (M ⁻¹ s ⁻¹)	$k_d \times 10^{-2}$ (s ⁻¹)	K_d (nM)
4E-BP1	10	0.44 ± 2	0.82 ± 0.8	17 ± 4
	15	0.51 ± 2	0.96 ± 0.9	17 ± 2
	20	0.62 ± 3	1.3 ± 0.2	21 ± 7
	25	0.82 ± 3	2.1 ± 0.4	26 ± 6
	30	1.3 ± 0.4	3.2 ± 0.5	24 ± 5
eIF4G	10	1.8 ± 0.3	1.8 ± 0.7	9.8 ± 0.7
	15	1.7 ± 0.5	2.2 ± 0.4	12 ± 2
	20	1.7 ± 0.3	3.5 ± 0.7	24 ± 4
	25	1.7 ± 0.3	4.8 ± 0.9	29 ± 6
	30	2.0 ± 0.2	10 ± 2	54 ± 11
KKR-4E-BP1	25	2.0 ± 0.09	15 ± 2	77 ± 7
4E-BP1 (R51-N64)	10	1.5 ± 0.03	0.69 ± 0.5	4.7 ± 0.5
	15	1.0 ± 0.2	0.93 ± 0.7	9.3 ± 1
	20	1.2 ± 0.2	1.3 ± 0.2	11 ± 1
	25	1.1 ± 0.1	1.9 ± 0.5	17 ± 0.4
	30	1.1 ± 0.1	3.1 ± 0.2	27 ± 2
Linear sTIP-04	10	1.5 ± 0.04	3.4 ± 0.4	23 ± 2
	15	2.3 ± 0.2	7.4 ± 2	32 ± 7
	20	2.6 ± 0.2	15 ± 0.8	57 ± 2
	25	2.0 ± 0.1	12 ± 2	62 ± 6
	30	1.9 ± 0.2	18 ± 0.7	92 ± 6

Table S2. Statistical significance between 4E-BP1 (R51–N64) and the 4E-BP1/eIF4G peptides at each temperature tested (ns = not significant)

Temperature (°C)	k_a	k_d	K_d
10	<0.0001 / 0.1340 (****/ns)	0.0691 / 0.0248 (ns/*)	0.0009 / <0.0001 (***/****)
15	0.0154 / 0.0707 (* / ns)	0.6541 / 0.0006 (ns/***)	0.0009 / 0.0548 (***/ns)
20	0.0213 / 0.2397 (* / ns)	0.6581 / 0.0011 (ns/**)	0.0596 / 0.0072 (ns/**)
25	0.1241 / 0.0053 (ns/**)	0.5435 / 0.0015 (ns/**)	0.0459 / 0.0567 (* / ns)
30	0.5132 / <0.0001 (ns/****)	0.7772 / 0.0011 (ns/**)	0.2739 / 0.0052 (ns/**)

Table S3. Statistical significance between 4E-BP1 and eIF4G peptides at each temperature tested (ns = not significant)

Temperature (°C)	k_a	k_d	K_d
10	<0.0001 (****)	0.0023 (**)	0.0004 (***)
15	0.0002 (***)	<0.0001 (****)	<0.0001 (****)
20	0.0008 (***)	<0.0001 (****)	0.8094 (ns)
25	<0.0001 (****)	<0.0001 (****)	0.6555 (ns)
30	0.0018 (**)	<0.0001 (****)	<0.0001 (****)

Table S4. Tabulated SPR results from Figures 4 and S11

Peptide	[NaCl] (mM)	$k_a \times 10^6$ ($M^{-1}s^{-1}$)	$k_d \times 10^{-2}$ (s^{-1})	K_d (nM)
4E-BP1	225	0.88 ± 3	2.3 ± 0.5	25 ± 6
	500	0.80 ± 3	5.5 ± 0.2	29 ± 1
	1000	2.0 ± 0.4	1.6 ± 0.7	7.9 ± 1
eIF4G	225	1.7 ± 0.3	4.6 ± 0.6	27 ± 5
	500	2.7 ± 0.8	15 ± 6	65 ± 4
	1000	5.3 ± 0.1	27 ± 7	51 ± 14
4E-BP1 (R51-N64)	225	1.1 ± 0.1	1.9 ± 0.05	17 ± 4
	500	0.94 ± 0.5	3.1 ± 0.4	23 ± 2
	1000	1.2 ± 0.2	8.6 ± 2	57 ± 3
Linear sTIP-04	225	2.0 ± 0.1	12.3 ± 2	62 ± 6
	1000	0.15 ± 0.4	0.25 ± 0.1	14 ± 2

Table S5. Statistical significance between 4E-BP1 and eIF4G peptides at each salt concentration tested (ns = not significant)

[NaCl] (mM)	k_a	k_d	K_d
225	0.0045 (**)	0.0012 (**)	0.6391 (ns)
500	0.0002 (***)	0.0012 (**)	0.0072 (**)
1000	0.0003 (***)	0.0404 (*)	0.0113 (*)

Table S6. Statistical significance between 4E-BP1 (R51–N64) and the 4E-BP1/eIF4G peptides at each salt concentration tested (ns = not significant)

[NaCl] (mM)	k_a	k_d	K_d
225	0.2453 / 0.0325 (ns/*)	0.2924 / 0.0009 (ns/****)	0.0746 / 0.0249 (ns/*)
500	0.5352 / <0.0001 (ns/****)	0.2090 / <0.0001 (ns/****)	0.2129 / 0.0023 (ns/**)
1000	0.0631 / 0.0004 (ns/****)	0.1110 / 0.0347 (ns/*)	0.0123 / 0.9001 (* / ns)

Table S7. Statistical significance between eIF4G and **linear sTIP-04** peptides at each temperature tested (ns = not significant)

Temperature (°C)	k_a	k_d	K_d
10	0.1252 (ns)	0.0156 (*)	<0.0001 (****)
15	0.0873 (ns)	0.0044 (**)	0.0029 (**)
20	0.0016 (**)	<0.0001 (****)	<0.0001 (****)
25	0.1410 (ns)	0.0007 (****)	0.0010 (****)
30	0.6702 (ns)	0.0007 (****)	0.0015 (**)

Table S8. Statistical significance between **linear sTIP-04** and the eIF4G/4E-BP1 peptides at each salt concentration tested (ns = not significant)

[NaCl] (mM)	k_a	k_d	K_d
225	0.3146 / 0.0010 (ns/**)	0.0039 / 0.0363 (**/*)	0.0045 / 0.0040 (**/**)
1000	0.0002 / 0.0040 (****/**)	0.0363 / 0.1282 (* / ns)	0.0227 / 0.2529 (* / ns)

Table S9. Statistical significance between **HCS-4E-BP1** and the control at each concentration tested in the m⁷GDP cap affinity chromatography assay (ns = not significant)

[HCS-4E-BP1] (μM)	eIF4G	4E-BP1
1.0	0.0333 (*)	0.0366 (*)
2.5	0.0117 (*)	0.0019 (**)
5.0	0.0028 (**)	0.0014 (**)

Table S10. Statistical significance between **sTIP-04** and the control at each concentration tested in the m⁷GDP cap affinity chromatography assay (ns = not significant)

[sTIP-04] (μM)	eIF4G	4E-BP1
1.0	0.0928 (ns)	0.1434 (ns)
2.5	0.0285 (*)	0.0372 (*)
5.0	0.0227 (*)	0.0276 (*)